Inorg. Chem. **2009**, *48*, 3848−3856

Synthesis, Crystal and Electronic Structures, and Physical Properties of the Novel Compounds $LaR_4Mo_{36}O_{52}$ (R = Dy, Er, Yb, and Y) Containing Infinite Chains of Trans-Edge-Shared Mo_6 Octahedra and Mo_2 Pairs and Rectangular Mo_4 Clusters with Triple Mo−Mo Bonds

N. Barrier,[†] B. Fontaine,[‡] S. Pierrefixe,[‡,§] R. Gautier,[‡] and P. Gougeon*[,‡]

Laboratoire CRISMAT, UMR CNRS 6508, 6, Boulevard Maréchal Juin 14050 CAEN Cedex 4, France, and Sciences Chimiques de Rennes, UMR CNRS 6226, Ecole Nationale Supérieure de Chimie de Rennes, Université de Rennes 1, Avenue du Général Leclerc, 35042 Rennes, France

Received October 13, 2008

The novel quaternary reduced molybdenum oxides $LaR_4Mo_{36}O_{52}$ (R = Dy, Er, Yb, and Y) have been synthesized with solid-state reactions at 1400 °C for 48 h in sealed molybdenum crucibles. The crystal structure was determined on a single crystal of $LaEr_4Mo_{36}O_{52}$ by X-ray diffraction. $LaEr_4Mo_{36}O_{52}$ crystallizes in the tetragonal space group $I\bar{4}$ with two formula units per cell and the following lattice parameters: $a = 19.8348(2)$ and $c = 5.6594(1)$ Å. The Mo network is dominated by infinite chains of trans-edge-shared Mo_6 octahedra, which coexist with Mo_2 pairs and rectangular Mo_4 clusters. The Mo−Mo distances within the infinite chains range from 2.5967(7) to 2.8529(8) Å and from 2.239(3) to 2.667(2) Å in the Mo_2 pairs and rectangular Mo_4 clusters, respectively. The Mo−O distances are comprised between 1.993(7) and 2.149(7) Å, as usually observed in these types of compound. The La^{3+} and Er^{3+} ions are in a square-prismatic [LaO_8] and a tricapped trigonal-prismatic [ErO_9] environment of oxygen atoms, respectively. The La−O distances range from 2.555(6) to 2.719(6) Å and the Er−O ones from 2.260(6) to 2.469(5) Å. Theoretical calculations allow the determination of the optimal electron count of both motifs in the title compound. Weak interactions occur between neighboring dimetallic and tetrametallic clusters and between trans-edge-sharing infinite chains and dimers and tetramers. The presence of rectangular clusters is favored on the basis of theoretical considerations. Single-crystal resistivity measurements show that $LaEr_4Mo_{36}O_{52}$ is metallic between 4.2 and 300 K, in agreement with the band structure calculations. Magnetic susceptibility measurements indicate that the oxidation state of the magnetic rare earths is +3, and there is an absence of localized moments on the Mo network.

Introduction

The formation of clusters and infinite chains by metal−metal bonding is a common feature of many compounds containing early transition metals in low oxidation states.[1] This is particularly well exemplified by the reduced molybdenum oxides that offer the widest array of clusters and infinite chains in solid-state chemistry up to the present time. Thus, 14 different clusters with nuclearity going from 2 in the Mo_2 pairs to 24 in the tricluster Mo_7−Mo_{10}−Mo_7[2] and eight different infinite chains are known to date in reduced molybdates. Although most of the crystal structures of the latter compounds contain only one type of cluster or chain, some of them present up to four different types of clusters or chains. For example, in $Pr_4Mo_9O_{18}$[3] coexist Mo_3, Mo_7, Mo_{13}, and Mo_{19} clusters, and in $R_4Mo_{18}O_{32}$,[4] we have three types of infinite chains with Mo_2 pairs, rhomboidal Mo_4, and octahedral Mo_6 clusters as repeat units. The diversity of the

* To whom correspondence should be addressed. E-mail: patrick.gougeon@univ-rennes1.fr.
† Laboratoire CRISMAT.
‡ Université de Rennes 1.
§ Present adress: Afdeling Theoretische Chemie, Scheikundig Laboratorium der Vrije Universiteit, De Boelelaan 1083, 1081 HV Amsterdam, The Netherlands.

(1) (a) Simon, A. *Angew. Chem., Int. Ed.* **1988**, *27*, 159–185. (b) SimonA. In *Clusters and Colloids*; Schmid, G., Ed.; VCH: Weinheim, Germany, 1994; pp 373−458.
(2) (a) Tortelier, J.; Gougeon, P. *Acta Crystallogr.* **1996**, *C 52*, 1862. (b) Tortelier, J.; Gougeon, P.; Ramanujachary, K. V.; Greenblatt, M. *Mater. Res. Bull.* **1998**, *8*, 1151.
(3) Tortelier, J.; Gougeon, P. *Inorg. Chem.* **1998**, *37* (24), 6229–6236.
(4) (a) Gougeon, P.; Gall, P.; Mc Carley, R. E. *Acta Crystallogr.* **1991**, *C47*, 2026. (b) Gall, P.; Gougeon, P.; Greenblatt, M.; McCarroll, W. H.; Ramanujachary, K. V. *J. Solid State Chem.* **1997**, *134*, 45.

10.1021/ic801942d CCC: $40.75
Published on Web 03/19/2009

structural arrangements of the clusters and chains in reduced molybdates gives rise to a wide variety of electrical and magnetic behaviors as well as interesting phenomena at low temperatures. For example, in the KMo_4O_6[5] and $R_4Mo_{18}O_{32}$[4] (R = Sm, Gd → Yb) compounds, metal−insulator transitions are observed at 50 and 90 K, respectively. The RMo_5O_8 (R = La → Gd) compounds containing bioctahedral Mo_{10} clusters show resistivity anomalies that could be due to charge density waves[6] and magnetic properties that are also varied, with the appearance of ferromagnetic and antiferromagnetic orders as well as spin-glass-like behavior.[7] In the RMo_8O_{14} (R = La, Ce, Pr, Nd, Sm)[8] compounds, a paramagnetic moment due to the Mo_8 clusters is observed, and at low temperatures, antiferromagnetic or ferromagnetic interactions are also found, either between clusters or between paramagnetic clusters and magnetic rare earths.[9] The Mo−Mo bonds in the above metal−metal bonded units range generally from 2.40 to 2.85 Å. The shortest Mo−Mo distances are observed in the dimer Mo_2 occurring in $La_5Mo_4O_{16}$ (2.406 Å),[10] $La_2Mo_2O_7$ (2.418 Å),[11] $Y_5Mo_2O_{12}$[12] (2.496 Å), and MoO_2[13] (2.511 Å). In the latter four compounds, the Mo_2 pairs are surrounded by 10 oxygen atoms to form Mo_2O_{10} groups consisting of two octahedral MoO_6 units sharing an edge. Shorter Mo−Mo distances of 2.138 Å, corresponding to a quadruple bond, are observed in the chloride $K_4Mo_2Cl_8 \cdot 2H_2O$.[14] In contrast to the oxides, the Mo_2 pairs are located in a distorted cube of chlorine atoms to form Mo_2Cl_8 units. Here, we report the synthesis, crystal and electronic structures, and electrical resistivity and magnetic measurements of the new series of compounds $LaR_4Mo_{36}O_{52}$ (R = Dy, Er, Yb and Y) in which very short Mo−Mo bonds of about 2.23 Å are observed in addition to infinite linear chains of trans-edge-sharing Mo_6 octahedra.

Experimental Section

Synthesis. Single crystals of the $LaR_4Mo_{36}O_{52}$ (R = Dy, Er, Yb, and Y) compounds were prepared from powdered mixtures of MoO_3 (Strem Chemicals, 99.9%), Mo (Cime bocuze, 99.99%), and R_2O_3 (R = La, Dy, Er, Yb, Y) (Strem Chemicals, 99.999%) with the nominal composition $LaRMo_{16}O_{28}$. Before use, the Mo powder was heated under a hydrogen flow at 1000 °C for 6 h and the rare-earth oxides were prefired at temperatures between 700 and 1000 °C overnight and left at 600 °C before weighing them. The mixtures were pressed into pellets (ca. 5 g) and loaded into molybdenum crucibles, which were previously outgassed at about 1500 °C for 15 min under a dynamic vacuum of about 10^{-5} Torr. The Mo crucibles were subsequently sealed under a low argon pressure using an arc welding system. The samples were heated at a rate of 300 °C/h to 1400 °C for 48 h and then cooled at 100 °C/h down to 1100 °C, at which point the furnace was shut down and allowed to cool to room temperature. We have thus obtained a black microcrystalline powder with single crystals of $LaR_4Mo_{36}O_{52}$, which grew in the form of black needles with a square cross-section. X-ray powder diffraction experiments revealed that the samples are always composed of two phases: $LaMo_8O_{14}$ and $LaR_4Mo_{36}O_{52}$. Attempts to synthesize monophasic powders of the $LaR_4Mo_{36}O_{52}$ (R = Dy, Ho, Er, Tm, Yb, Lu, and Y) compounds starting from the stoichiometric composition were unsuccessful and led to mixtures of $LaMo_8O_{14}$ and $R_4Mo_{18}O_{32}$ (R = Dy, Ho, Er, Tm, Yb, and Lu).[4,8] The unit-cell parameters of the $LaR_4Mo_{36}O_{52}$ (R = Dy, Er, Yb, and Y) compounds determined from single-crystal X-ray diffraction data are given in Table 1.

Table 1. Unit-Cell Parameters for the $LaR_4Mo_{36}O_{52}$ (R = Dy, Er, Yb, and Y) Compounds

compounds	a (Å)	c (Å)	V (Å^3)
$LaDy_4Mo_{36}O_{52}$	19.8681(2)	5.66180(1)	2234.95(5)
$LaEr_4Mo_{36}O_{52}$	19.8348(2)	5.6594(1)	2226.51(5)
$LaYb_4Mo_{36}O_{52}$	19.8136(4)	5.6587(1)	2221.48(8)
$LaY_4Mo_{36}O_{52}$	19.8595(6)	5.6610(1)	2232.78(10)

Single-Crystal Structure Determination. A needlelike crystal of $LaEr_4Mo_{36}O_{52}$ with approximate dimensions of 0.75 × 0.029 × 0.019 mm^3 was selected for data collection. Intensity data were collected on a four-circle Nonius Kappa CCD diffractometer equipped with a CCD area detector. The experiment was conducted using graphite-monochromatized Mo Kα (λ = 0.71073 Å) X-ray radiation at room temperature. A total of 35 107 reflections were recorded on 328 frames using $\Delta\omega$ = 1.8° rotation scans with an X-ray exposure time of 36 s and a crystal-to-detector distance of 25 mm. Reflection indexing, Lorentz-polarization correction, peak integration, and background determination were performed using the program DENZO from the Kappa CCD software package.[15] An empirical absorption correction was applied with the SORTAV program.[16] Examination of the data set did not show any supplementary systematic extinctions other than that corresponding to the *I*-type lattice and revealed that the Laue class was 4/*m*, leading to the possible space groups *I*4, $I\bar{4}$, and *I*4/*m*. The structure was solved in space group $I\bar{4}$ by direct methods using SIR97,[17] which reveals the rare-earth atoms, all of the Mo atoms forming infinite chains of trans-edge-sharing Mo_6 octahedra, and a part of the oxygen atoms. After refinement of the latter model using SHELXL-97,[18] a difference Fourier synthesis revealed the remaining oxygen atoms and two peaks 1.62 Å from each other that we assigned to

(5) Ramanujachary, K. V.; Greenblatt, M.; Jones, E. B.; McCarroll, W. H. *J. Solid State Chem.* **1993**, *102*, 69.
(6) Gall, P; Gougeon, P.; Greenblatt, M.; Jones, E. B.; McCarroll, W. H.; Ramanujachary, K. V. *Croat. Chem. Acta* **1995**, *68*, 849.
(7) Gall, P.; Noël, H.; Gougeon, P. *Mater. Res. Bull.* **1993**, *28*, 1225.
(8) (a) Leligny, H.; Ledésert, M.; Labbé, Ph.; Raveau, B.; McCarroll, W. H. *J. Solid State Chem.* **1990**, *87*, 35–43. (b) Gougeon, P.; McCarley, R. E. *Acta Crystallogr.* **1991**, *C47*, 241. (c) Leligny, H.; Labbé, Ph.; Ledesert, M.; Hervieu, M.; Raveau, B.; McCarroll, W. H. *Acta Crystallogr.* **1993**, *B49*, 444–454. (d) Kerihuel, G.; Gougeon, P. *Acta Crystallogr.* **1995**, *C51*, 787. (e) Kerihuel, G.; Gougeon, P. *Acta Crystallogr.* **1995**, *C51*, 1475. (f) Kerihuel, G.; Tortelier, J.; Gougeon, P. *Acta Crystallogr.* **1996**, *C52*, 2389. (g) Tortelier, J.; Gougeon, P. *Inorg. Chem.* **1998**, *37*, 6229–6236.
(9) Gougeon, P.; Kerihuel, G.; Noël, H.; Greedan, J. Presented at the Vth European Conference on Solid State Chemistry, Montpellier, France, September 4−7, 1995.
(10) Ledésert, M.; Labbé, Ph.; McCarroll, W. H.; Leligny, H.; Raveau, B. *J. Solid State Chem.* **1993**, *105*, 143–150.
(11) Moini, A.; Subramanian, M. A.; Clearfield, A.; Di Salvo, F. J.; McCarroll, W. H. *J. Solid State Chem.* **1987**, *66*, 136.
(12) Torardi, C. C.; Fecketter, C.; McCarroll, W. H.; Di Salvo, F. J. *J. Solid State Chem.* **1985**, *60*, 332.
(13) Magneli, A.; Anderson, G.; Holmberg, B.; Kihlborg, L. *Anal. Chem.* **1952**, *24*, 1998.
(14) Brencic, J. V.; Cotton, F. A. *Inorg. Chem.* **1969**, *8*, 7.
(15) (a) *COLLECT*; KappaCCD Software, Nonius BV: Delft, The Netherlands, 1998. (b) Otwinowski, Z.; Minor, W. In *Methods in Enzymology*; Carter, C. W., Jr., Sweet, R. M., Eds.; Academic Press: New York, 1997; Vol. *276*, pp 307−326.
(16) Blessing, R. H. *Acta Crystallogr.* **1995**, *A51*, 33–38.
(17) Altomare, A.; Burla, M. C.; Camalli, M.; Cascarano, G. L.; Giacovazzo, C.; Guagliardi, A.; Moliterni, A. G. G.; Polidori, G.; Spagna, R. *J. Appl. Crystallogr.* **1999**, *32*, 115–119.
(18) Sheldrick, G. M. *SHELXL97*; University of Göttingen: Göttingen, Germany, 1997.

Table 2. X-Ray Crystallographic and Experimental Data for $LaEr_4Mo_{36}O_{52}$

formula	$LaEr_4Mo_{36}O_{52}$
fw (g mol^{-1})	5093.79
space group	$I\bar{4}$
a (Å)	19.8348(2)
c (Å)	5.6594(1)
V (Å^3)	2226.52(5)
Z	2
ρ_{calcd} (g cm^{-3})	7.598
T (°C)	20
λ (Å)	0.71073 (Mo Kα)
μ (cm^{-1})	182.25
R_1[a] (on all data)	0.0399
wR_2[b] (on all data)	0.0940

[a] $R_1 = \sum ||F_o| - |F_c|| / \sum |F_o|$. [b] $wR_2 = \{\sum [w(F_o^2 - F_c^2)^2] / \sum [w(F_o^2)^2]\}^{1/2}$, $w = 1/[\sigma^2(F_o^2) + (0.0279P)^2 + 64.3224P]$ where $P = [\max(F_o^2,0) + 2F_c^2]/3$.

Mo atoms according to geometric considerations. Refinement of this new model taking into account the positional and anisotropic atomic displacement parameters for all atoms as well as the site occupancy factors for Mo9 and Mo10 because of the unrealistic distance between the latter two atoms converged to a residual $R(F_o^2) = 0.0363$ for the 5576 reflections having $F_o^2 > 2\sigma(F_o^2)$ with residual electron densities of +3.955 and −2.732 e.A^{-3}. Refinements of the occupancy factors for the Mo9 and Mo10 sites yielded values of 0.50(1) and 0.50(1), respectively, and consequently an overall stoichiometry of $LaEr_4Mo_{36}O_{52}$. Because of the partial occupation of the Mo9 and Mo10 atoms, we made long-exposure rotation scans along the three crystallographic axes. The latter did not reveal any superlattice reflection. Refinement of Flack's x parameter[19] indicated that the crystal studied was racemically twinned, as often observed in inorganic compounds. A summary of the X-ray crystallographic and experimental data is presented in Table 2. Atomic coordinates and equivalent isotropic displacement parameters as well as selected interatomic distances are reported in Tables 3 and 4, respectively.

Electrical Resistivity Measurements. The ac resistivity was measured on single crystals at 80 Hz with a current amplitude of 20 μA using standard four-probe techniques between 290 and 4.2 K. Ohmic contacts were made by attaching molten indium ultrasonically.

Magnetic Susceptibility Measurements. Susceptibility data were collected on powder samples or batches of single crystals in the temperature range between 4.2 and 300 K on a SHE-906 SQUID magnetosusceptometer at an applied field of 0.5 T. The data were subsequently corrected for the diamagnetic contribution of the sample holder.

Extended Hückel Calculations. Molecular and periodic calculations have been carried out within the extended Hückel formalism[20] with the programs CACAO and YAeHMOP, respectively.[21,22] The exponents (ξ) and the valence shell ionization potentials (H_{ii} in eV) were (respectively): +2.275 and −32.3 for O 2s, +2.275 and −14.8 for O 2p, +1.956 and −8.34 for Mo 5s, and +1.921 and −5.24 for Mo 5p. H_{ii} values for Mo 4d were set equal to −10.50. A linear combination of two Slater-type orbitals of exponents $\zeta_1 = 4.542$ and $\zeta_2 = 1.901$ with the weighting coefficients $c_1 = c_2 = 0.5898$ was used to represent the Mo 4d atomic orbitals. The density of states (DOS) and crystal orbital overlap populations (COOP) were obtained using a set of 18 k points.

Results and Discussion

Crystal Structure. A projection of the crystal structure of $LaEr_4Mo_{36}O_{52}$ on the (001) plane is shown in Figure 1a. It can be described as blocks of four infinite trans-edge-sharing Mo_6 octahedral cluster chains parallel to the c axis that are interconnected through O atoms and Mo_2O_8 units. Within the blocks, the infinite chains which consist of trans-edge-shared Mo_6O_{12} building units are linked to each other by trigonally bonded sp^2-type oxygen atoms, as observed in $NaMo_4O_6$[23] (Figure 1b), to form tunnels of a square cross-section in which the lanthanum atoms reside. These $NaMo_4O_6$-type blocks are then interlinked through O1 atoms that are coordinated by four waist Mo atoms in an approximately square-planar symmetry (Figure 1c). This type of interlinkage is similar to those found in other oxide phases, such as NbO,[24] $Mg_3Nb_6O_{11}$,[25] $MM'Mo_4O_7$ (M = Al, Ti, Fe, Sc; M' = Zn, Fe, Mo),[26] MMo_8O_{10} (M = Li, Zn),[27] and $Mn_{1.5}Mo_8O_{11}$.[28,29]

Compared to the structure of $NaMo_4O_6$, the most striking feature within the Mo infinite chains present in $LaR_4Mo_{36}O_{52}$ is the pairwise distortion occurring between the apex molybdenum atoms Mo3, Mo4, Mo7, and Mo8, as shown in Figure 2. This pairing, previously observed in $ZnMo_8O_{10}$,[27] $Gd_4Mo_{18}O_{32}$,[4] $R_4Mo_4O_{11}$,[30] and, more recently, $Mn_{1.5}Mo_8O_{11}$,[29] is accompanied by alternating short and long bond distances between the molybdenum atoms of the common edges Mo1−Mo2 and Mo5−Mo6 of the Mo_6 octahedra. The short Mo−Mo bond distances between the apical molybdenum atoms are 2.5967(7) Å for Mo3−Mo7 and 2.6010(7) Å for Mo4−Mo8, while the long ones, which are essentially nonbonding, are 3.0650(7) and 3.0607 (7) Å. The waist Mo atom bond distances are shorter (Mo1−Mo2: 2.6128 (8) Å) when the apical−apical interaction is weaker (i.e., Mo3−Mo7) and longer (Mo5−Mo6: 2.8180 (8) Å) when the interaction between the apex Mo atoms is stronger (i.e., Mo4−Mo8). It results from the distortion that the waist molybdenum atoms are bonded to seven molybdenum atoms and the apex molybdenum atoms to five molybdenum atoms. In addition, the apex Mo atoms are surrounded by five oxygen atoms in a square-pyramidal environment and the atoms of the shared edges by four oxygen atoms forming a flattened tetrahedron. The Mo−O distances range from 1.993(7) to 2.149(7) Å, as usually observed in the reduced molybdenum oxides. This distortion from the regular bonding seen in $NaMo_4O_6$, in which the distances between apical molybdenum atoms as well as between waist atoms are identical (2.8618(2) Å), results from the different electron counts per Mo_4 fragment observed in both structural types. Indeed, it has been shown

(19) Flack, H. D. *Acta Crystallogr.* **1983**, *A39*, 876.
(20) (a) Hoffmann, R. *J. Chem. Phys.* **1963**, *39*, 1397. (b) Whangbo, M.-H.; Hoffmann, R. *J. Am. Chem. Soc.* **1978**, *100*, 6093.
(21) Mealli, C.; Proserpio, D. *J. Chem. Educ.* **1990**, *67*, 399.
(22) Landrum, G. A. *YAeHMOP, Yet Another extended Hückel Molecular Orbital Package*, release 2.0; Cornell University: Ithaca, NY, 1997.
(23) Torardi, C. C.; McCarley, R. E. *J. Am. Chem. Soc.* **1979**, *101*, 3963.
(24) Bowman, A. L.; Wallace, T. C.; Yarnell, J. L.; Wenzel, R. G. *Acta Crystallogr.* **1966**, *21*, 843.
(25) Burnus, R.; Koehler, J.; Simon, A. *Z. Naturforsch.* **1987**, *42*, 536.
(26) Mc Carley, R. E. *Philos. Trans. R. Soc. London, Ser. A* **1982**, *308*, 41.
(27) Lii, K. H.; McCarley, R. E.; Kim, S.; Jacobson, R. A. *J. Solid State Chem.* **1986**, *64*, 347.
(28) Carlson, C. D.; Brough, L. F.; Edwards, P. A.; McCarley, R. E. *J. Less Common Met.* **1989**, *156*, 325.
(29) Gall, P.; Gougeon, P. *Acta Crystallogr.* **2007**, *E62*, 55.
(30) Gall, P.; Barrier, N.; Gautier, R.; Gougeon, P. *Inorg. Chem.* **2002**, *41*, 2879.

Table 3. Atomic Coordinates, Site Occupancy Factors, and Equivalent Isotropic Displacement Parameters (Å^2) for $LaEr_4Mo_{36}O_{52}$[a]

atoms	SOF	τ	x	y	z	U(eq)
Er	8g	1	0.590414(14)	0.210754(14)	0.99217(6)	0.01137(6)
La	2a	1	1	0	1	0.01518(13)
Mo1	8g	1	0.76581(3)	0.17006(3)	0.74740(14)	0.00865(9)
Mo2	8g	1	0.80267(3)	0.04360(3)	0.75059(15)	0.00868(9)
Mo3	8g	1	0.68988(3)	0.07775(3)	1.01929(13)	0.00883(9)
Mo4	8g	1	0.87776(3)	0.13595(3)	0.01710(13)	0.00843(9)
Mo5	8g	1	0.76470(3)	0.17472(3)	0.24773(14)	0.00839(9)
Mo6	8g	1	0.80446(3)	0.03833(3)	0.24686(15)	0.00873(9)
Mo7	8g	1	0.68801(3)	0.08131(3)	0.47789(12)	0.00881(9)
Mo8	8g	1	0.87765(3)	0.13185(3)	0.47647(12)	0.00879(10)
Mo9	8g	0.501(4)	0.55496(7)	−0.01099(7)	0.2348(4)	0.0134(3)
Mo10	8g	0.500(4)	0.55531(7)	−0.01127(7)	0.7636(4)	0.0129(3)
O1	8g	1	0.7519(2)	0.2506(2)	0.4984(17)	0.0129(7)
O2	8g	1	0.6645(3)	0.1473(3)	0.7544(14)	0.0108(8)
O3	8g	1	0.8625(3)	0.2040(3)	0.7391(13)	0.0109(8)
O4	8g	1	0.9733(2)	0.1717(2)	0.0085(15)	0.0126(8)
O5	8g	1	0.5838(3)	0.0610(3)	0.0029(15)	0.0201(10)
O6	8g	1	0.6625(3)	0.1554(3)	0.2421(14)	0.0113(8)
O7	8g	1	0.8602(3)	0.2122(3)	0.2545(13)	0.0099(8)
O8	8g	1	0.8198(2)	−0.0303(2)	0.5084(13)	0.0107(7)
O9	8g	1	0.5527(3)	−0.0865(2)	−0.0005(15)	0.0148(8)
O10	8g	1	0.7032(3)	0.0081(3)	0.7405(12)	0.0099(8)
O11	8g	1	0.9046(3)	0.0678(3)	0.7499(13)	0.0091(7)
O12	8g	1	0.9079(3)	0.0590(3)	0.2385(12)	0.0111(9)
O13	8g	1	0.7050(3)	−0.0005(3)	1.2536(13)	0.0102(8)

[a] U(eq) is defined as one-third of the trace of the orthogonalized U_{ij} tensor.

by Hughbanks and Hoffmann from extended Hückel band structure calculations[31] that, for electron counts greater than 13 e^- per Mo_4 repeat unit, as found in $NaMo_4O_6$, the excess electrons occupy antibonding states involving $d_{x^2-y^2}$ orbitals of the apex Mo atoms, and consequently distortions are expected. In $LaEr_4Mo_{36}O_{52}$, by using the empirical bond length−bond strength relationship developed by Brown and Wu[32] for Mo−O bonds $s(Mo-O) = [d(Mo-O)/1.882]^{-6}$, we found a value of 13.6(2) e^- per Mo_4 repeat unit, which explained why the infinite trans-edge-sharing Mo_6 octahedral cluster chains are distorted.

The 50% occupation of the Mo9 and Mo10 sites leads to the formation of either Mo_2 pairs or rectangular Mo_4 clusters. The Mo_2 pairs can be in an eclipsed position or rotated with respect to each other by 90°. The three possibilities for the arrangement of the Mo atoms are shown in Figure 3. The Mo−Mo distances are 2.223(3) and 2.239(3) Å in the Mo_2 pairs and along the edges of the rectangular Mo_4 clusters perpendicular to the *c* axis and 2.6666(17) Å parallelly. The very short distances of about 2.23 Å are consistent with the presence of triple bonds, while the longer one corresponds to a single bond (see Theoretical Study section). The Mo9 and Mo10 atoms of the dimer and tetramer are surrounded by four oxygen atoms, forming thus Mo_2O_8 or Mo_4O_{12} units (Figure 4). The Mo_2O_8 unit can be described as a slightly distorted cube of oxygen atoms, within which the Mo_2 pair is centered along one pseudo-4-fold axis. Such a unit is similar to those encountered in the chloride compounds such as $K_4Mo_2Cl_8 \cdot 2H_2O$,[14] $K_2Re_2Cl_8 \cdot 2H_2O$,[33] or $(NH_4)_3Tc_2Cl_8 \cdot 2H_2O$[34] prepared in acidic solution. However, in the latter three compounds, the very short M−M bond lengths (2.139(4), 2.241(7), and 2.13(1) Å, respectively) clearly indicate the presence of quadruple bonds, as confirmed by theoretical calculations. The Mo_4O_{12} unit results from the face-sharing of two Mo_2O_8 units, the two Mo_2 pairs being parallel (Figure 4b). Although some examples of the rectangular tetranuclear Mo_4L_{12} unit are known in metal−organic compounds, it is totally new to solid chemistry. The existence of a rectangular Mo_4L_{12} unit was first reported by McGinnis et al. in 1978 with the compound $Mo_4Cl_8(PEt_3)_4$.[35] In the latter compound, the Mo−Mo distances in the short and long dimensions of the rectangle are 2.211(3) and 2.901(2) Å, corresponding to a triple and a single bond, respectively. The Mo−O bonds distances in both units range from 2.003(7) to 2.088(7) Å.

While in $NaMo_4O_6$ the Na atoms occupy all distorted tetragonal-prismatic sites in the tunnels formed by the inner oxygen atoms of the four infinite chains, in $LaEr_4Mo_{36}O_{52}$, the La^{3+} ions occupy only half of the distorted tetragonal-prismatic sites within the $NaMo_4O_6$-type blocks (Figure 5). Each La^{3+} ion is displaced from the center of its tetragonal prismatic site and thus has four nearest oxygen atoms at 2.555(6) Å and four furthest ones at 2.719(6) Å. In addition, there are four interchain oxygen atoms O4, as next-nearest neighbors to lanthanum at 3.447(3) Å. The average La−O bond distance is 2.635 Å, which is larger than the value of 2.56 Å expected from the sum of the ionic radii of La^{3+} (CN 8) and O^{2-} (CN 4).[15] The distance between two close La^{3+} ions is 3.5735(9) Å.

The environments of the Er^{3+} ions consist of nine oxygen atoms placed at the vertices of a distorted tricapped trigonal prism, the triangular faces being perpendicular to *c*. As for the lanthanum, the vertices of the trigonal prism correspond to intrachain oxygen atoms, while the capping O atoms

(31) Hughbanks, T.; Hoffmann, R. *J. Am. Chem. Soc.* **1983**, *105*, 3528.
(32) Brown, I. D.; Wu, K. K. *Acta Crystallogr.* **1976**, *B32*, 1957.
(33) Cotton, F. A.; Harris, C. B. *Inorg. Chem.* **1965**, *4*, 330.
(34) Bratton, W. K.; Cotton, F. A. *Inorg. Chem.* **1970**, *9*, 789.
(35) McGinnis, R. N.; Ryan, T. R.; McCarley, R. E. *J. Am. Chem. Soc.* **1978**, *100*, 7900.

Table 4. Main Interatomic Distances (Å) in $LaEr_4Mo_{36}O_{52}$

Er−O2	2.357(7)	Er−O8	2.469(5)
Er−O3	2.384(7)	Er−O10	2.361(6)
Er−O6	2.291(6)	Er−O13	2.294(6)
Er−O7	2.260(6)		
La−O11 (×4)	2.719(6)	La−O12 (×4)	2.555(6)
Mo1−Mo2	2.6128(8)	Mo5−Mo6	2.8180(8)
Mo1−Mo3	2.8264(8)	Mo5−Mo7	2.7285(9)
Mo1−Mo4	2.7782(9)	Mo5−Mo8	2.7237(8)
Mo1−Mo5	2.8294(8)	Mo6−Mo2	2.8108(8)
Mo1−Mo5	2.8332(8)	Mo6−Mo2	2.8529(8)
Mo1−Mo5	3.1376(7)	Mo6−Mo3	2.7268(9)
Mo1−Mo7	2.7941(9)	Mo6−Mo4	2.7484(9)
Mo1−Mo8	2.8012(9)	Mo6−Mo5	2.8180(8)
Mo2−Mo1	2.6128(8)	Mo6−Mo7	2.7878(9)
Mo2−Mo3	2.7886(9)	Mo6−Mo8	2.6901(9)
Mo2−Mo4	2.8016(9)	Mo7−Mo1	2.7941(9)
Mo2−Mo6	2.8108(8)	Mo7−Mo2	2.8485(9)
Mo2−Mo6	2.8529(8)	Mo7−Mo3	2.5967(7)
Mo2−Mo7	2.8485(9)	Mo7−Mo3	3.0650(7)
Mo2−Mo8	2.7718(9)	Mo7−Mo5	2.7285(9)
Mo3−Mo1	2.8264(8)	Mo7−Mo6	2.7878(9)
Mo3−Mo2	2.7886(9)	Mo8−Mo1	2.8012(9)
Mo3−Mo5	2.7521(8)	Mo8−Mo2	2.7718(9)
Mo3−Mo6	2.7268(9)	Mo8−Mo4	2.6010(7)
Mo3−Mo7	2.5967(7)	Mo8−Mo4	3.0607(7)
Mo3−Mo7	3.0650(7)	Mo8−Mo5	2.7237(8)
Mo4−Mo1	2.7782(9)	Mo8−Mo6	2.6901(9)
Mo4−Mo2	2.8016(9)	Mo9−Mo9 (×2)	1.582(2)
Mo4−Mo5	2.7063(8)	Mo9−Mo9	2.223(3)
Mo4−Mo6	2.7484(9)	Mo9−Mo10	2.6666(17)
Mo4−Mo8	2.6010(7)	Mo9−Mo10	2.9928(17)
Mo4−Mo8	3.0607(7)	Mo10−Mo9	2.6666(17)
Mo5−Mo1	2.8332(8)	Mo10−Mo10 (×2)	1.591(2)
Mo5−Mo1	3.1376(7)	Mo10−Mo10	2.239(3)
Mo5−Mo3	2.7521(8)	Mo10−Mo9	2.9928(17)
Mo5−Mo4	2.7063(8)		
Mo1−O1	2.147(7)	Mo6−O12	2.093(6)
Mo1−O1	2.149(7)	Mo6−O13	2.118(5)
Mo1−O2	2.059(5)	Mo6−O4	1.993(7)
Mo1−O3	2.033(6)	Mo6−O8	2.033(6)
Mo2−O4	2.015(7)	Mo7−O2	2.093(8)
Mo2−O8	2.035(6)	Mo7−O6	2.049(6)
Mo2−O10	2.096(5)	Mo7−O9	2.096(5)
Mo2−O11	2.077(5)	Mo7−O10	2.100(6)
Mo3−O2	2.099(6)	Mo7−O13	2.088(6)
Mo3−O5	2.131(5)	Mo8−O3	2.085(7)
Mo3−O6	2.063(7)	Mo8−O7	2.058(6)
Mo3−O10	2.114(6)	Mo8−O8	2.065(4)
Mo3−O13	2.064(6)	Mo8−O11	2.073(6)
Mo4−O3	2.096(7)	Mo8−O12	2.065(6)
Mo4−O4	2.025(5)	Mo9−O5	2.022(8)
Mo4−O7	2.052(6)	Mo9−O5	2.075(7)
Mo4−O11	2.097(6)	Mo9−O9	2.005(7)
Mo4−O12	2.064(6)	Mo9−O9	2.061(7)
Mo5−O1	2.073(7)	Mo10−O5	2.051(7)
Mo5−O1	2.083(7)	Mo10−O5	2.088(7)
Mo5−O6	2.064(5)	Mo10−O9	2.003(7)
Mo5−O7	2.034(5)	Mo10−O9	2.052(7)

belong to the environment of the Mo_2 pairs. The Er−O distances range from 2.260(6) to 2.384(7) Å for the oxygen atoms forming the trigonal prism, and the distances between the erbium and the capping atoms are comprised between 2.469(5) and 3.220(4) Å (Figure 6).

Theoretical Study. Within the EHTB approximation, rare-earth atoms of $LaEr_4Mo_{36}O_{52}$ can be treated as La^{3+} and Er^{3+} ions, giving their three valence electrons. Consequently, the electronic structure of the title compound is approximated by that of the $[Mo_{36}O_{52}]^{15-}$ lattice. The two crystallographic structures envisioned on the basis on X-ray diffraction have been considered.

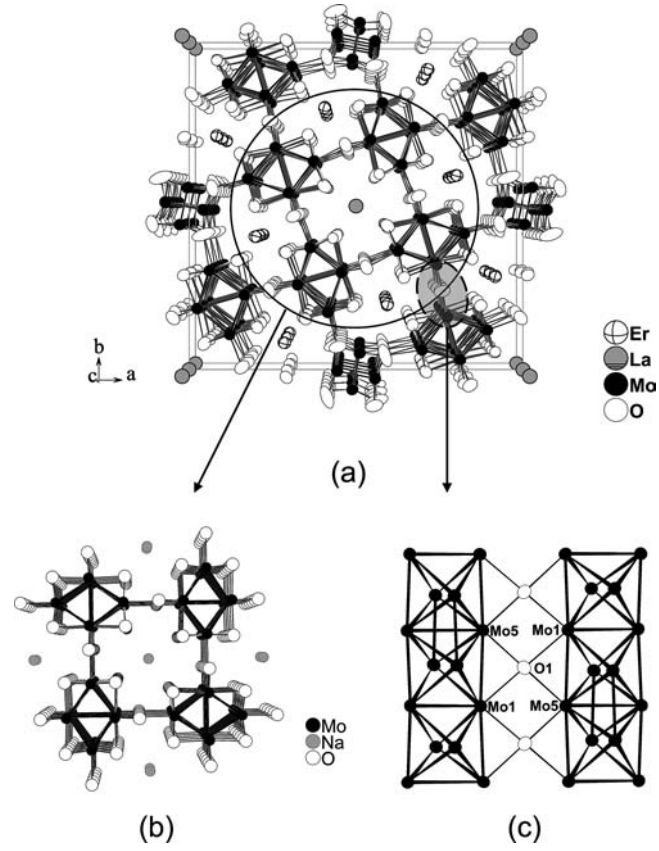

Figure 1. (a) The crystal structure of $LaEr_4Mo_{36}O_{52}$ as viewed down the *c* axis, parallel to the direction of the chain growth. Thick lines denote Mo−Mo bondings, and thin lines denote Mo−O bondings. Ellipsoids are drawn at the 97% probability level. (b) Crystal structure of $NaMo_4O_6$. (c) Interconnection of the $NaMo_4O_6$-type blocks in $LaEr_4Mo_{36}O_{52}$.

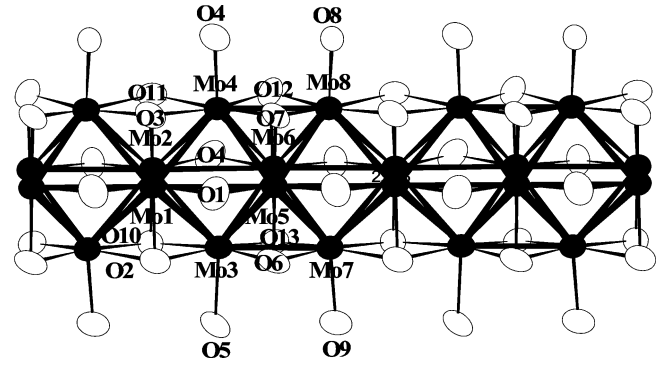

Figure 2. A section of one molybdenum oxide cluster chain. The repeat unit comprises two Mo_6 octahedra.

As a first approach of the electronic structure, one can consider separately the infinite chains of edge-shared octahedral clusters and the dimers and tetramers of both structures. In order to study the band structure of these latter ones, molecular orbital (MO) diagrams of M_2L_8 and M_4L_{12} units (M = transition metal, L = ligand) with idealized D_{4h} and D_{2h} geometries, respectively, are shown in Figure 7. Starting from two square-planar, D_{4h}, ML_4 fragments, the MO diagram of the D_{4h} M_2L_8 dimer is easily built. As shown in Figure 7, the electronic structure of a bimetallic cluster with a triple M−M bond is characterized by one σ and two π bonding MOs. These MOs are low enough in energy that their electronic occupation is favorable. This is not the case

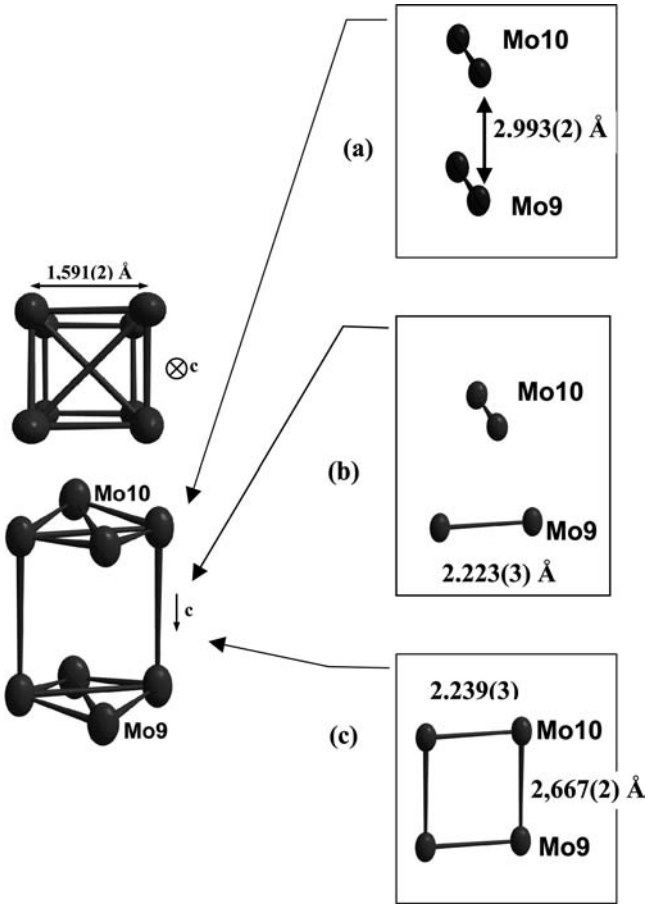

Figure 3. Different arrangements of the Mo9 and Mo10 atoms in $LaEr_4Mo_{36}O_{52}$.

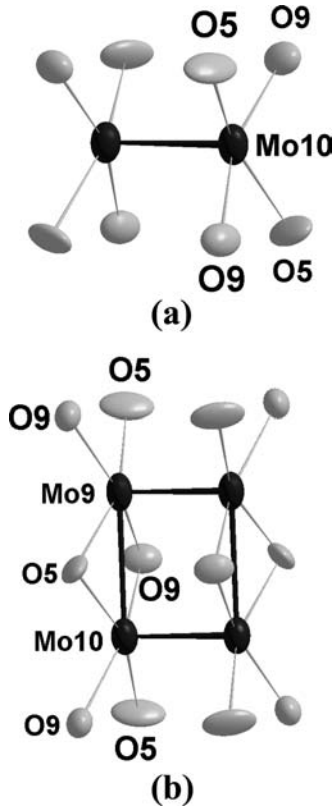

Figure 4. The (a) Mo_2O_8 and (b) Mo_4O_{12} cluster units in $LaEr_4Mo_{36}O_{52}$.

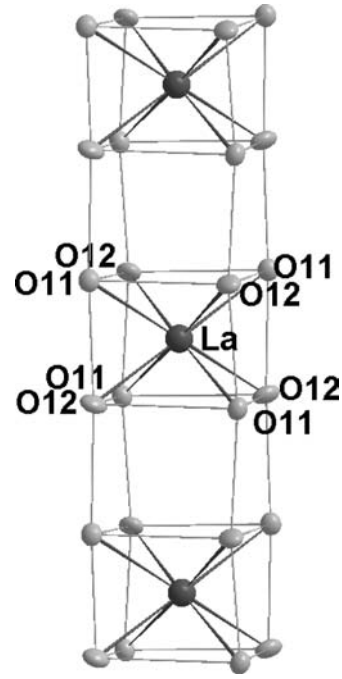

Figure 5. A view perpendicular to the c axis of $LaEr_4Mo_{36}O_{52}$ showing the arrangement of the La^{3+} cations within a square cross-section channel.

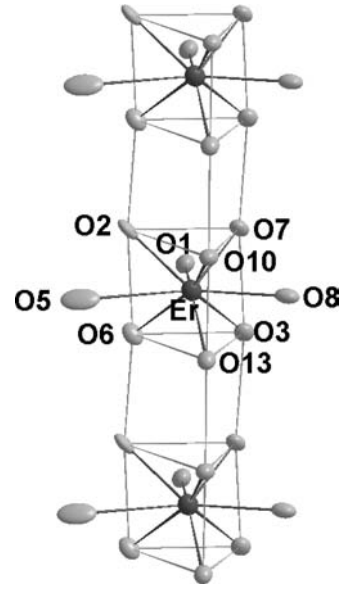

Figure 6. A view perpendicular to the c axis of $LaEr_4Mo_{36}O_{52}$ showing the arrangement of the Er^{3+} cations within a triangular cross-section channel.

of the corresponding σ and π out-of-phase combinations. In a triply bonded bimetallic system, the two δ frontier molecular orbitals (FMOs) of each ML_4 fragment interact weakly so that the resulting MOs are more or less nonbonding. Therefore, the favored metallic electron (ME) count of such a cluster is equal to 10.[36] Although these two δ MOs of the M_2L_8 cluster are roughly nonbonding along the M≡M bond, they are well oriented for a significant interaction with another bimetallic M_2L_8 fragment in order to constitute a M_4L_{12} ($M_4L_8L_{8/2}$) rectangular cluster. The MO diagram of

(36) Albright, T. A.; Burdett, J. K.; Whangbo, M.-H. *Orbital Interaction in Chemistry*; John Wiley and Sons: New York, 1985.

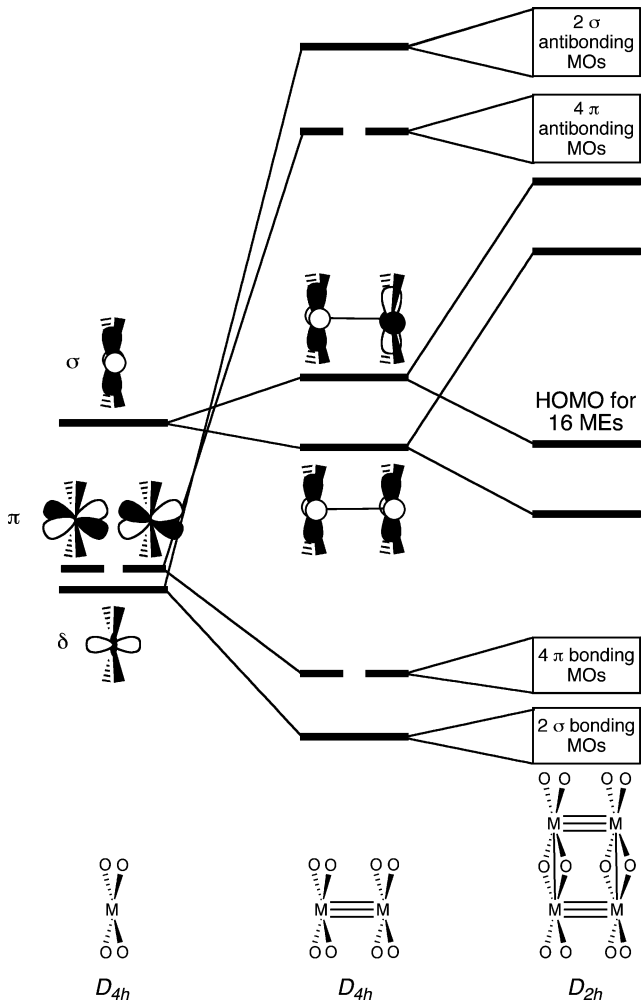

Figure 7. Qualitative MO diagrams based on EH calculations for the idealized Mo_2O_8 and Mo_4O_{12} clusters. The FMOs of the MoO_4 fragment are shown of the left-hand side.

such a cluster lies on the right part of Figure 7. Bonding and antibonding σ and π MOs of the M_2L_8 fragments are hardly perturbed by the interaction, whereas each of the two δ MOs of one M_2L_8 unit interacts strongly with the δ MOs of the same symmetry of the other bimetallic cluster. Applying the closed-shell requirement to this rectangular cluster leads therefore to the favored 16 MEs count. Mo−Mo and Mo≡Mo calculated overlap populations are equal to 0.152 and 0.952, respectively. These values are consistent with the presence of two single and two triple metal−metal bonds in the rectangular cluster. Molecular EH calculations for Mo_2O_8 and Mo_4O_{12} species as found in the title compound have confirmed this qualitative analysis.

How are the MO patterns of the Mo_2O_8 and Mo_4O_{12} clusters perturbed when the one-dimensional stacking is considered? Band structure and COOPs for Mo−Mo bonds of both arrangements are sketched in Figure 8. The unit cell of the title compound has been considered. Only the molybdenum and oxygen atoms belonging to the dimers or tetramers have been taken into account. The dispersion diagram of the $Mo_2O_{8/2}$ chains shows five broad bands. The three lowest large bands that lie between −11.8 and −10.4 eV derive from the σ and π bonding MOs of the dimer. The other broad band that lies between −10.1 and −9.4 eV is derived from δ bonding MOs of the triply bonded dimer. The Mo−Mo COOP curve suggests that the Mo−Mo bonds are optimized for 8 MEs per $Mo_2O_{8/2}$ motif since the flat bands that lie around −9.4 eV show some significant antibonding character (cf. Figure 8). If two extra electrons are added, that is 10 MEs per $Mo_2O_{8/2}$ motif, occupied bands are separated from vacant antibonding bands by an energetic gap of ca. 0.5 eV. The band structure of the $Mo_4O_4O_{8/2}$ chains shows that only weak interactions occur between Mo_4 rectangular motifs since all bands are rather flat. Indeed, Mo−Mo overlap populations between tetramers are lower than 0.01. The optimal ME count for such a one-dimensional system remains equal to 16 per $Mo_4O_4O_{8/2}$ motif, as shown by the Mo−Mo COOP curve (cf. Figure 8).

The electronic structure of infinite chains of edge-shared octahedral clusters have been studied using EHTB calculations.[31] It has been shown that the optimal ME count for a regular infinite chain is equal to 13 per Mo_4 units and that distortions of the chains are expected for a greater ME count. Recently, periodic density functional calculations were carried out in order to study the band structure of $R_4Mo_4O_{11}$ compounds (R = Nd−Tm and Y) that contain the same distorted infinite chains as in the title compound.[30] It has been shown that the distortion observed in these compounds stabilizes the structure for 14 MEs, compared to the regular chain. For this electron count, a small band gap separates the bonding occupied bands from vacant bands.

In order to study the interaction between the edge-sharing chains and the dimer and tetramers, EHTB calculations have been carried out for both $[Mo_{36}O_{52}]^{15-}$ arrangements. These calculations allow the comparison between the two electronic structures. DOS and Mo−Mo COOP curves are sketched in Figure 9. For both calculations, the densities of states at the Fermi level suggest a metallic behavior. This was confirmed by the electrical resistivity measurements carried out on a single crystal of $LaEr_4Mo_{36}O_{52}$ along the *c* axis (direction of the chain growth), which show a metallic behavior between 4.2 and 300 K with a room resistivity of 2.1 mΩ·cm (Figure 10). The Mo−Mo COOP curves of the infinite chain and the associated projected DOS (not shown here) are very similar for both crystal structures. Metal−metal bonding in these chains is optimal for both crystal structures since almost all bonding and nonbonding bands are occupied and antibonding bands are vacant. Averaged Mo−Mo overlap populations within the chain are equal to 0.22 in both calculations. The COOP curve for metal−metal bonds in the rectangular cluster shows that metal bonding is almost optimized; only one weakly Mo−Mo bonding band is vacant. In the case of the presence of the dimer in the title compound, some bands that show some Mo−Mo bonding character are vacant. If one consider that the ME count of the infinite chain remains the same in both calculations, Mo−Mo bonding in the oligomer is better optimized in the rectangular cluster than in the dimer since the optimal ME count is equal to 16 and 20 (2 × 10) in the tetramer and dimer, respectively, for the same number of metal atoms. This discussion, based on overlap considerations, would expand with more quantitative arguments. Unfortunately, attempts to calculate the density

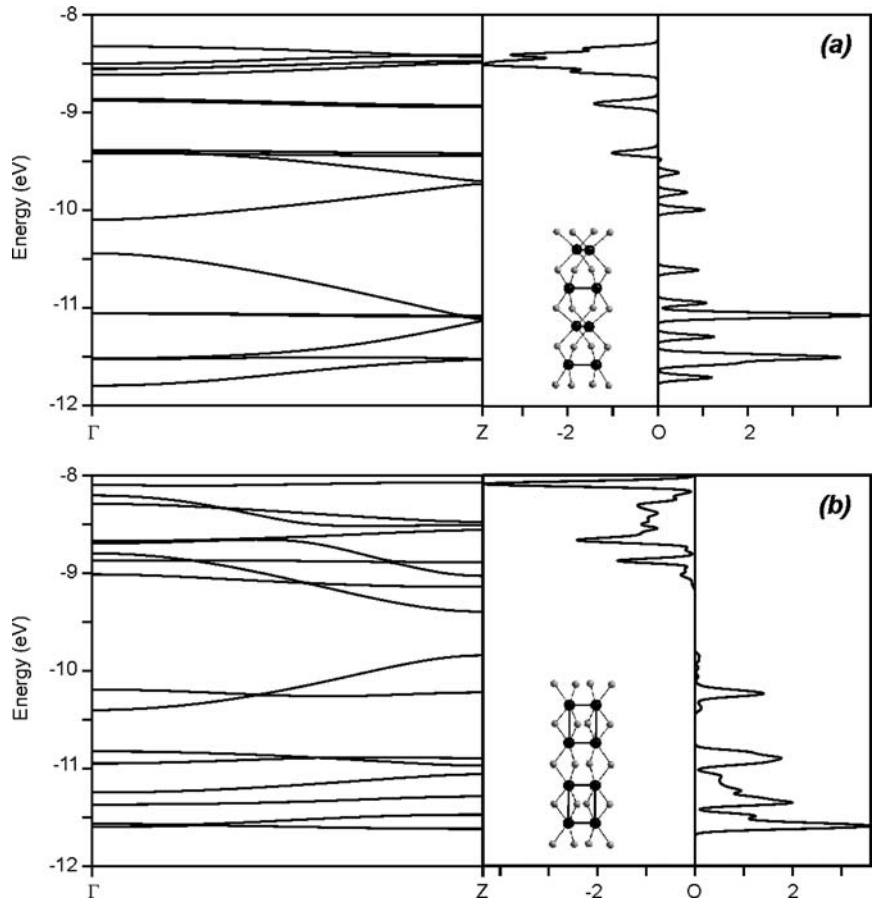

Figure 8. Band structure and Mo−Mo COOP curves for chains of (a) dimers and (b) tetramers.

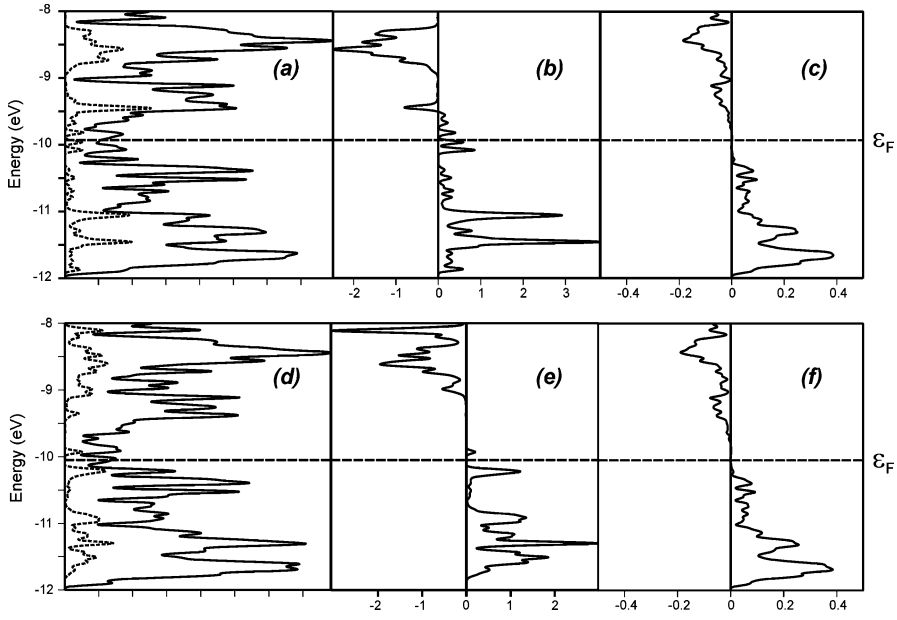

Figure 9. EHTB calculations for the $[Mo_{36}O_{52}]^{15-}$ structure with Mo_2 dimers: (a) total DOS (plain) and metal dimer projected DOS (dotted), (b) Mo−Mo COOP in the dimers, and (c) Mo−Mo COOP in the chain. Calculations with Mo_4 tetramers: (d) total DOS (plain) and metal tetramer projected DOS (dotted), (e) Mo−Mo COOP in the tetramers, and (f) Mo−Mo COOP in the chain.

functional theory band structure of both arrangements failed using the TB-LMTO-ASA program.[37]

Magnetic Properties. The temperature dependence of the molar magnetic susceptibility of $LaY_4Mo_{36}O_{52}$ is shown in Figure 11. The susceptibility of this compound is nearly temperature-independent in the range 100−300 K with a value of about 7.5×10^{-4} emu/mol. This behavior is consistent with the absence of localized moments on the Mo atom network. The low-temperature upturn could be attributed to small amounts of paramagnetic impurities often present in the starting reactants. Figure 12 shows the temperature dependence of the inverse susceptibility below 300

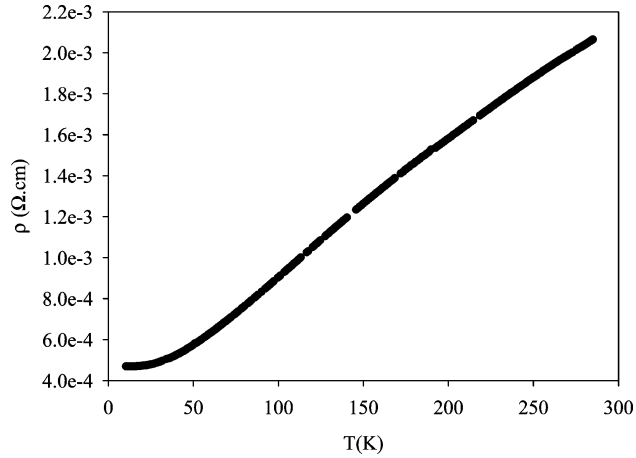

Figure 10. Temperature dependence of the electrical resistivity for $LaEr_4Mo_{36}O_{52}$.

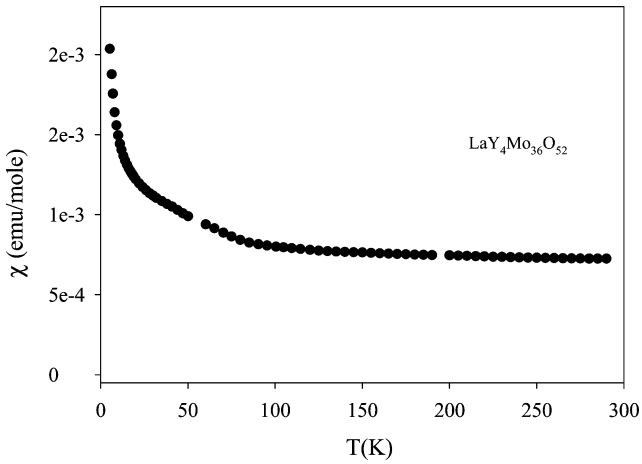

Figure 11. Temperature dependence of the susceptibility for $LaY_4Mo_{36}O_{52}$.

K for $LaDy_4Mo_{36}O_{52}$ and $LaEr_4Mo_{36}O_{52}$. The magnetic susceptibilities of $LaDy_4Mo_{36}O_{52}$ and $LaEr_4Mo_{36}O_{52}$ follow the Curie−Weiss behavior over the 4.2−300 K temperature range. The susceptibility data were fitted to a Curie−Weiss law, $\chi = C/(T - \theta)$, in the 4.2−300 K temperature range. From the fits, we could deduce effective moments, μ_{eff}, equal to 10.61 μ_B and 9.54 μ_B, which are in excellent agreement with the values of 10.63 μ_B and 9.57 μ_B expected for trivalent Dy and Er ions, respectively, from Hund's rule.[40] No signature of magnetic ordering was found down to 4.2 K for both compounds.

Concluding Remarks

This work reports the synthesis, the single crystal structure determination, and the electronic structure of the novel $LaR_4Mo_{36}O_{52}$ (R = Dy, Er, Yb, and Y) compounds. A single-crystal study revealed that their crystal structure contains infinite chains of trans-edge-shared Mo_6 octahedra, which

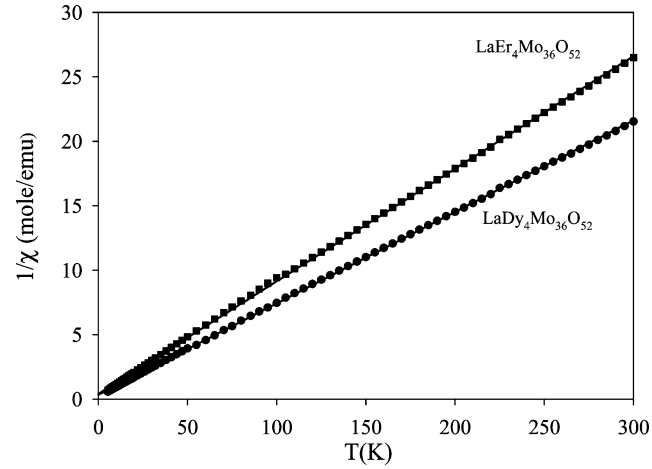

Figure 12. Reciprocal susceptibilities of $LaDy_4Mo_{36}O_{52}$ and $LaEr_4Mo_{36}O_{52}$ as a function of the temperature. Data were taken under an applied field of 0.5 T. The solid lines represent the fit to a Curie−Weiss law in the range of 4.2−300 K.

coexist with Mo_2 pairs and rectangular Mo_4 clusters. Extended Hückel calculations are more in favor of the existence of tetrametallic clusters. The lack of long-range order, since no evidence was found for any superstructure or for lower symmetry, makes it impossible to determine the true local structure. Consequently, additional studies using a combination of extended X-ray absorption fine structure and total neutron diffraction as used previously for Li_2MoO_3, $LiMoO_2$, and $Li_4Mo_3O_8$[38,39] would be perhaps helpful in ascertaining the true local structure in these materials and determining the true nuclearity of the molybdenum clusters present in these compounds. Finally, the arrangement of the trans-edge-shared Mo_6 octahedra chains is similar in $LaR_4Mo_{36}O_{52}$ and $NaMo_4O_6$. The existence of compounds isomorphous with $LaR_4Mo_{36}O_{52}$ can be envisaged by replacing the La^{3+} cations by either monovalent cations such as Na^+, K^+, or In^+ or divalent cations such as Sr^{2+}, Ba^{2+}, Sn^{2+}, or Pb^{2+} in the four-sided channels since the $NaMo_4O_6$-type structure is observed for the latter cations. On the other hand, we can also expect a $NaMo_4O_6$-type structure with the lanthanum.

Supporting Information Available: X-ray crystallographic file for $LaEr_4Mo_{36}O_{56}$, in CIF format, is available. This material is available free of charge via the Internet at http://pubs.acs.org.

IC801942D

(37) Tank, R. W.; Jepsen, O.; Burkhardt, A.; Andersen, O. K. *The STUTTGART TB-LMTO-ASA program*, *version 4.7*; Max-Planck-Institut fur Festkorperforschung: Stuttgart, Germany, 1999.
(38) Hibble, S. J.; Fawcett, I. D. *Inorg. Chem.* **1995**, *34*, 500.
(39) Hibble, S. J.; Fawcett, I. D.; Hannon, A. C. *Acta Crystallogr.* **1997**, *B53*, 604.
(40) Van Vleck, J. H. *Electric and Magnetic Susceptibilities*; Oxford University Press: New York, 1932; p 243.